Analysis of a one-component sorption in a single adsorbent particle by the orthogonal collocation method
III. Kinetics of n-heptane adsorption on molecular sieve Calsit 5*

P. RAJNIAK and A. ŽEMLIČKA

Department of Chemical Engineering, Slovak Technical University, CS-812 37 Bratislava

Received 1 March 1984

This paper deals with a theoretical and experimental investigation of adsorption kinetics. The adsorption on molecular sieve Calsit 5 of n-heptane from a nitrogen stream is studied experimentally in a differential bed. The influence of particle size, gas inlet concentration and temperature and linear gas velocity is investigated. The mass transfer rate is calculated theoretically by means of three various models. A comparison between theory and experiments allows to determine both the apparent pore diffusivity and the apparent surface diffusivity. The results presented in this paper provide evidence for the existence of surface diffusion.

В работе описано теоретическое и экспериментальное изучение кинетики адсорбции. Адсорбция н-гептана из струи азота на молекулярном сите Calsit 5 была исследована экспериментально в дифференциальном слое. Изучалось влияние величины частиц, концентрации, температуры и линейной скорости тока газа. Скорость переноса вещества вычислялась теоретически с помощью трех различных моделей. Сравнение теории с экспериментом позволяет определить кажущиеся коэффициенты диффузии в порах и поверхностной диффузии. Приведенные в работе результаты являются доказательством существования поверхностной диффузии.

The purpose of this work was to investigate the rate of adsorption on porous particles of one component of a gaseous mixture and to provide the information necessary for the prediction of the behaviour of a fixed bed adsorber.

Porous adsorbents, catalysts, and ion exchangers contain irregular networks of pores of various sizes and shapes. The description of transport processes in such solids is inherently difficult owing to the complex and largely unknown nature of

* Presented at the Statewide Seminar "Adsorption Processes in Environmental Protection", Kočovce, May 24—26, 1983.

the pore network and because, depending on the dimensions of pores, the mechanism of mass transport may be due to bulk diffusion, Knudsen diffusion, and surface diffusion. Consequently most models for diffusion in porous solids are approximate. The type of porous solids which is of particular interest here has a bidisperse pore distribution. Commercial molecular sieves consist of small crystals of synthetic zeolite pelleted with a clay binder. The kinetics of sorption is governed by two distinct diffusional resistances: the macropore resistance of the pellet and the micropore resistance of zeolite crystals. In order to interpret kinetic data for such systems it is in general necessary to take account of both diffusional processes although, under certain conditions, one or the other of the resistances may be rate-controlling [1]. *Wakao* and *Smith* [2] have proposed a "random pore" model to describe diffusion in porous solids of a bidisperse pore structure. The general problem of diffusion in solids of a bidisperse pore structure has been discussed by *Ruckenstein et al.* [3] who derived a theoretical expression for the transient sorption curve under a linear isotherm approximation for a macroporous spherical particle composed of small uniform microporous microspheres. This is a useful model for a molecular sieve pellet although the assumption that zeolite crystals may be treated as an assemblage of uniform spherical particles is not always a very good approximation [4].

Transport mechanism

The adsorption of a compound from a solvent to and into an adsorbent is usually described by a two-step process: Transport through the "film" to the outer surface of the particle and diffusion into porous particle. The models used by various investigators differ basically in the description of the diffusional process within the adsorbent particle.

The complex transport mechanisms of the adsorbate in the adsorbent are often simplified by assuming that the transport is governed either by the diffusion of the species in the pore fluid, described as a normal diffusion in a fluid, or by the diffusion in the solid or on the pore surfaces. The last two mechanisms are treated as one, since they can be treated in the same way mathematically [5] with the assumption that the accumulation of the adsorbate within the pores has been neglected. As the two transport processes, *i.e.* pore (macropore) diffusion and surface diffusion are parallel, the combined diffusion rate will be the sum of the pore diffusion rate and surface diffusion rate. Reaction rate at the adsorptive sites is usually not rate-limiting, which shows that local equilibrium exists between the fluid and the solid phase everywhere in the particle. The removal of the dissolved compound from bulk fluid to the adsorption sites inside the adsorbent can then be described, under nonisothermal conditions, by one of the following two transport mechanisms or by the combination of both:

1. Mass and heat transfer in the "film" surrounding the particle

The molar flux equation is

$$\boldsymbol{J}_F = h_M(c_o - c_R) \tag{1}$$

and the heat flux equation is

$$\boldsymbol{H}_F = h(T_o - T_R) \tag{2}$$

where $\boldsymbol{J}_F$ is the flux of the adsorbate through the external surface layer, $\boldsymbol{H}_F$ is the heat flux through the external surface layer, and h, h_M are heat and mass transfer coefficients, respectively.

2. Mass and heat transport within the particle

The total molar flux of the adsorbate is assumed to consist of two contributions

$$\boldsymbol{J}_I = \boldsymbol{J}_P + \boldsymbol{J}_A = -D_P\nabla c - D_A\nabla a \tag{3}$$

The right-side terms are the fluxes of the adsorbate by gaseous diffusion and surface diffusion with D_P as the effective pore diffusion coefficient, and with D_A as the effective surface diffusion coefficient. For nonisothermal particles a heat flux equation is also needed. Here the total heat flux in an isotropic particle is represented by the following model [6]

$$\boldsymbol{H}_I = \boldsymbol{J}_P h_P + \boldsymbol{J}_A h_A - \lambda_e\nabla T = -D_P h_P\nabla c - D_A h_A\nabla a - \lambda_e\nabla T \tag{4}$$

that is, as a sum of convective and conductive terms, h_P and h_A being partial molar enthalpies and λ_e the effective conductivity of the porous medium.

Mathematical models

At an unsteady state, the fluxes in a porous particle formally satisfy the mass and enthalpy balances

$$\frac{\partial a_t}{\partial t} = -\nabla \ \boldsymbol{J}_I \tag{5}$$

$$\frac{\partial h_t}{\partial t} = -\nabla \ \boldsymbol{H}_I \tag{6}$$

subject to appropriate boundary conditions. Here $a_t = a + \varepsilon c$ is the total loading of the particle and $h_t = h_s + ah_A + \varepsilon c h_P$ is the total molar enthalpy of the particle. The total loading of the particle is practically equal to solid loading a, since $a \gg \varepsilon c$.

I. Heterogeneous diffusion model

By introducing eqns (*3*) and (*4*), differential mass and enthalpy balances (*5*) and (*6*) can be transformed, after some manipulation, into

$$\frac{\partial a}{\partial t} = \nabla \cdot D_P \nabla c + \nabla \quad D_A \nabla a \tag{7}$$

$$\varrho C_p \frac{\partial T}{\partial t} = \nabla \quad \lambda_e \nabla T + (-\Delta H) \left[\frac{\partial a}{\partial t} - \nabla \quad D_A \nabla a \right] \tag{8}$$

The corresponding uniform boundary conditions at the surface may now be states as

$$\boldsymbol{J}_I = \boldsymbol{J}_F \quad \text{and} \quad \boldsymbol{H}_I = \boldsymbol{H}_F \tag{9}$$

or

$$-D_P \nabla c - D_A \nabla a = h_M (c_R - c_o) \tag{10a}$$

$$\text{at } r = R \quad \text{for} \quad t > 0$$

$$-\lambda_e \nabla T - \Delta H D_A \nabla a = h(T_R - T_o) \tag{10b}$$

$$\nabla c = \nabla a = \nabla T = 0 \quad \text{at} \quad r = 0 \quad \text{for} \quad t > 0 \tag{11}$$

The initial conditions are

$$\begin{aligned} a &= a_i \\ c &= c_i^* \quad \text{at} \quad 0 \leqslant r \leqslant R \quad \text{for} \quad t = 0 \\ T &= T_i \end{aligned} \tag{12}$$

Here c_o and T_o are the properties of the bulk fluid phase and c_R and T_R are the corresponding values on the surface of the particle.

In this work equilibrium relationship of Langmuir type

$$a = a_s(T) \frac{K(T)P}{1 + K(T)P} \tag{13}$$

is used and together with eqns (*7*) and (*8*) and boundary and initial conditions (*9—12*) mathematically describes the heterogeneous diffusion model. According to this model, the adsorbent particle is regarded as a solid, interspersed with very small pores. Internal diffusion can occur simultaneously by pore (macropore) diffusion and by surface diffusion. The frequently used pore diffusion and surface diffusion models are special cases of the heterogeneous diffusion model.

II. Pore diffusion model

This model pictures the particle as consisting of a solid phase interspersed with pores, but with the adsorbate diffusing in the pore voids only, and the adsorption occurring at the internal surface. The adsorbed molecules are immobilized, $D_A = 0$, and can migrate only by desorbing first. The mass and heat balances and the

boundary conditions can be formally derived from eqns (*7—12*) by letting $D_A = 0$.

$$\frac{\partial a}{\partial t} = \nabla \quad D_P \nabla c \tag{14}$$

$$\varrho C_p \frac{\partial T}{\partial t} = \nabla \quad \lambda_e \nabla T - \Delta H \frac{\partial a}{\partial t} \tag{15}$$

Boundary conditions

$$-D_P \nabla c = h_M (c_R - c_o) \tag{16a}$$

$$\text{at} \quad r = R \quad \text{for} \quad t > 0$$

$$-\lambda_e \nabla T = h(T_R - T_o) \tag{16b}$$

Boundary conditions for $r = 0$, initial conditions and equilibrium relationship are as in (*11—13*), respectively.

III. Surface diffusion model

This model pictures the adsorption process as occurring at the outer surface of a pellet, followed by the diffusion of the adsorbate in the adsorbated state. In this homogeneous model, even though the pellets may be rather porous, there are no sinks for the adsorbate since it diffuses into them in the adsorbed state. The entire process might be pictured as an adsorption at the outer surface of the pellets followed by a sponge-like absorption of the adsorbate into them [7]. The relevant equations follow from eqns (*7—10*) by letting $D_P = 0$

$$\frac{\partial a}{\partial t} = \nabla \quad D_A \nabla a \tag{17}$$

$$\varrho C_p \frac{\partial T}{\partial t} = \nabla \quad \lambda_e \nabla T \tag{18}$$

Boundary conditions

$$-D_A \nabla a = h_M (c_R - c_o) \tag{19a}$$

$$\text{at} \quad r = R \quad \text{for} \quad t > 0$$

$$-\lambda_e \nabla T - \Delta H D_A \nabla a = h(T_R - T_o) \tag{19b}$$

Boundary conditions for $r = 0$, initial conditions and equilibrium relationship are in the form given in (*11—13*).

Solution and computing methods

a) Pore diffusion models

In the previous papers [8, 9] the method of orthogonal collocation has been used for the solution of isothermal and nonisothermal pore diffusion models in connection with the explicit Runge—Kutta—Merson technique to solve the resulting ordinary differential equations.

In this paper a more sophisticated integration technique, STIFF3 [10], is used and the computational time is fairly reduced. The solution of pore diffusion models with constant diffusivity is obtained by first transforming partial differential equations into ordinary differential equations by the orthogonal collocation method and then solving them using the STIFF3 routine.

Solutions $a(r, t)$ were integrated over the sphere volume by the numerical quadrature to give an average value of the total loading of particle $\bar{a}$ [8, 10].

b) Surface diffusion models

The procedure described above can be also used for the solution of isothermal and nonisothermal surface diffusion models. Another alternative would be to use a simplified model where computations are simpler. One simplified model is an isothermal surface diffusion model with the external diffusion neglected (Second Fick's law) and with constant diffusivity

$$\frac{\partial a}{\partial t} = D_A \nabla^2 a \tag{20}$$

Boundary conditions

$$a = a_o^* \quad \text{at } r = R \quad \text{for } t > 0 \tag{21}$$

$$\nabla a = 0 \quad \text{at } r = 0 \quad \text{for } t > 0 \tag{22}$$

Initial condition

$$a = 0 \quad \text{at } 0 \leqslant r \leqslant R \quad \text{for } t = 0 \tag{23}$$

An analytical solution of this equation, correct with the precision better than 10^{-4} up to $\bar{a}/a_o^* \leqslant 0.85$, has the form of

$$\frac{\bar{a}}{a_o^*} = 6 \sqrt{\frac{D_A t}{R^2}} - 3 \frac{D_A t}{R^2} \tag{24}$$

Experimental

The experiments were performed with the apparatus described in [11]. The experimental equipment which was used to produce a nitrogen stream of constant values of n-heptane concentration, flow rate and temperature, is also described in [11]. The nitrogen stream, which has constant properties, is led through a distributor with eight identical branches. Each branch consists of a tube with an off-valve, followed by one part of an earline (Fig. 1).

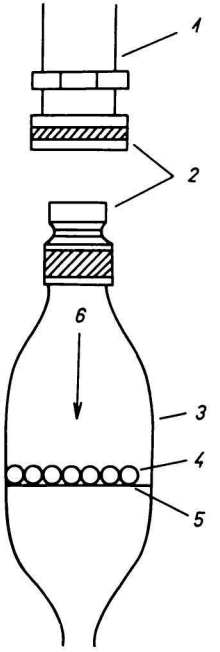

Fig. 1. The differential adsorbent bed.
1. One of the eight distributor branches; *2.* earline for quick mounting; *3.* glass vessel; *4.* one layer of molecular sieve; *5.* silver screen; *6.* gas mixture.

Its other part, permanently air-tight, is fastened to a glass vessel, in which one single layer of molecular sieve particles is placed on a silver screen. The earline allows very quick mounting and removal of the glass vessel. The time dependence of the adsorption is measured by weighing the glass vessel with its content on a Mettler balance ($m = 0.0001$ g) at a selected set of time values.

Results

The adsorption of n-heptane on molecular sieve Calsit 5 was investigated. In order to obtain experimental data for the evaluation we have performed experiments in the differential bed described above. The experiments were carried out with the following values of particle diameter d_P, inlet gas temperature T_o (initial bed temperature equals T_o in all experiments), inlet gas concentration c_o, and modified Reynolds' number Re_P

$d_P = 2.3$ mm; 2.9 mm
$T_o = 40$ °C; 56 °C
$c_o = 0.146$ mol m^{-3}; 0.361 mol m^{-3}; 0.548 mol m^{-3}
$Re_P = 77$; 1459; 3321
The exact values of these parameters are specified for each experiment in Table 1.

Evaluation of results

Intraparticle diffusivities may be evaluated by the superposition of model predictions onto experimental results obtained from single-solute tests in the differential bed by graphical comparison [12] or by nonlinear regression analysis [13]. An alternative method is to make the comparison at one point of the concentration transient with the aid of diagrams, for example at $\bar{a}/a_o^* = 0.4$ [14], or at $\bar{a}/a_o^* = 0.5$ [15], or at $\bar{a}/a_o^* = 0.66$ [16]. The drawback of making the comparison at a single value of $\bar{a}/a_o^*$ is that only one point of the whole sorption curve is used. This leads to a loss of information. It is doubtful, however, if more complicated methods will lead to a significantly better accuracy, and if they will warrant the extra effort, keeping in mind the inaccuracies of the experimental data. In this work the value of D_P or D_A, respectively, is found by reading the experimental value at $\bar{a}/a_o^*$ for $t = 10$ min (Table 1). From the corresponding abscisa on the theoretical curve the value of the apparent pore or surface diffusivity is found. The solutions of the isothermal and the nonisothermal pore diffusion model and of the isothermal surface diffusion model are plotted in order to make a comparison with the experimental results described above.

Table 1

Experimental conditions and results

Run	θ_o/°C	d_P / mm	c_o / mol m^{-3}	Re_P	Bi_M	$\left(\frac{\bar{a}}{a_o^*}\right)_{10}$	$D_P^* \cdot 10^6$ / m^2 s^{-1}	$D_A^* \cdot 10^{10}$ / m^2 s^{-1}
1	40	2.9	0.548	1459	11118	0.360	0.080	0.459
2	40	2.9	0.146	1459	5457	0.281	0.163	0.285
3	50	2.9	0.146	77	728	0.304	0.196	0.339
4	50	2.9	0.146	1459	4679	0.307	0.201	0.346
5	50	2.9	0.361	77	1209	0.359	0.118	0.492
6	50	2.9	0.361	1459	7405	0.371	0.127	0.531
7	50	2.9	0.548	77	1413	0.408	0.101	0.660
8	50	2.9	0.548	1459	9797	0.405	0.096	0.648
9	50	2.3	0.361	1459	7524	0.467	0.125	0.573
10	50	2.9	0.146	3321	7693	0.311	0.207	0.357
11	56	2.9	0.548	1459	7247	0.484	0.134	0.990
12	56	2.9	0.146	1459	3518	0.358	0.276	0.489

Table 1 shows estimated apparent pore diffusivities D_P^*, assuming nonisothermal pore diffusion model, eqns (*11*—*16*), and estimated apparent surface diffusivities D_S^*, assuming an isothermal surface diffusion model, eqns (*11*—*13*), (*17*—*19*), together with experimental conditions d_P, c_o, T_o, Re_P, the experimental values of $\bar{a}/a_o^*$ for $t = 10$ min, and Biot's number Bi_M for the pore diffusion model.

Discussion

The results showed that the differences in the apparent pore diffusivities, assuming isothermal and nonisothermal pore diffusion models, are less than 5 % (computed maximum temperature rise in the particle is in the range of 0.02—0.29 °C).

The values of the resulting Biot's number are in the range of 728—11 118. The differences in the estimated diffusivities for various modified Reynolds' numbers (Run *3* vs. Run *4*, Run *5* vs. Run *6*, Run *7* vs. Run *8*) are less than 7 %.

This means that the isothermal process can be taken into account while the external diffusion resistance can be neglected [9]. This was also the reason why the solution of the isothermal surface diffusion model, with the external diffusion neglected, eqn (*24*), could be used in evaluating the experimental data. Only one run (Run *9*) was carried out with particle diameter $d_P = 2.3 \times 10^{-3}$ m to compare the particle dimension influence on the rate of sorption. The estimated value of $D_p = 0.125 \times 10^{-6}$ m^2 s^{-1} is in good agreement with the value of $D_p =$

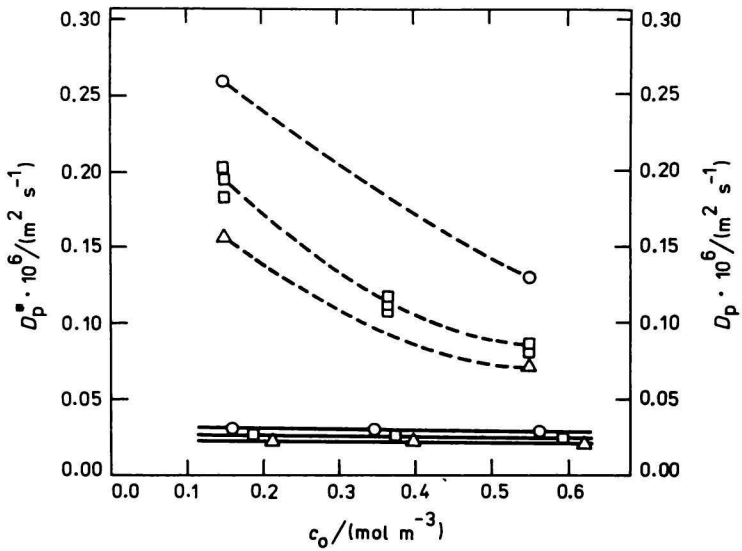

Fig. 2. Estimated apparent pore diffusivities D_P^* (– – –) and effective pore diffusivities D_P (———). × 40 °C; □ 50 °C; ○ 56 °C.

$= 0.127 \times 10^{-6}$ m^2 s^{-1} in Run 6. Fig. 2 shows estimated apparent pore diffusivities D_P^*. The values of D_P^* increase with increasing temperature as can be expected, but decrease with increasing fluid phase concentration. The latter discrepancy has been found by other authors as well [16] and is attributed unanimously to the surface diffusion. If this mechanism contributes to the internal mass transport, then the diffusive flux in the particle, eqn (3), expressed in terms of the concentration gradient in the fluid phase, is given (for the isothermal case) by

$$\mathbf{J}_I = -D_P \nabla c - D_A \nabla a = -\left(D_P + D_A \frac{\partial a}{\partial c}\right) \nabla c = -D_P^* \nabla c \qquad (25)$$

where apparent pore diffusivity D_P^* is

$$D_P^* = D_P + D_A \frac{\partial a}{\partial c} \qquad (26)$$

From this relationship it is obvious that lower values of the isotherm slope correspond to the values of D_P^*. For favourable isotherms the slope of the isotherm decreases with increasing equilibrium loading and increasing temperature as can be expected. In this case the apparent surface diffusivity is

$$D_A^* = D_A + D_P \frac{\partial c}{\partial a} \qquad (27)$$

Fig. 3 shows estimated apparent surface diffusivities D_A^*.

A combination of film, pore, and surface diffusion mechanisms involves two adjustable parameters, diffusivities D_P and D_A. These parameters cannot be

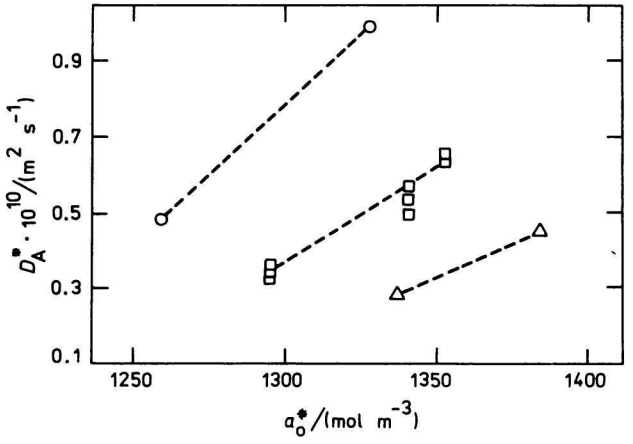

Fig. 3. Estimated apparent surface diffusivities D_A^* (– – –). × 40 °C; □ 50 °C; ○ 56 °C.

estimated independently of single solute tests. *Fritz et al.* [16] proposed a simple method for evaluating both diffusivities. The maximum magnitude of pore diffusivity can be precalculated from effective pore diffusivity D_P in eqn (*28*)

$$D_P = \frac{\varepsilon D_{BK}}{\mu} \quad \text{with} \quad \frac{1}{D_{BK}} = \frac{1}{D_B} + \frac{1}{D_K} \tag{28}$$

where D_B is gas-phase binary diffusivity (bulk diffusivity) and D_K is a "Knudsen diffusivity" [17]. Labyrinth factor μ is greater than one because of the tortuosity and constriction during mass transport in the particle. The value of $\mu = 1$ has been considered in this work, *i.e.* the maximum contribution due to pore diffusion. With this assumption, the diffusivities D_P are evaluated and compared with those estimated on the basis of pore diffusion model as shown in Fig. 2. The differences between curves are caused by the surface diffusion contribution. As can be seen, the relative importance of surface transport increases as both solid phase concentration and temperature decrease.

Conclusion

Attempt has been made to separate contributions from pore (macropore) and surface diffusion. The maximum contribution from pore diffusion is 34 % for the largest solid phase concentration and temperature, but for most data it is less than 20 %. Therefore, two models can be recommended for further consideration, *i.e.* the surface diffusion model and the heterogeneous diffusion model, which both include a contribution of surface diffusion.

The adsorption studies described here are the first step in an investigation of nonisothermal adsorption in the fixed bed. The next step is to compare theoretical and experimental results for adiabatic fixed bed adsorption using the results given above.

Symbols

a	adsorbate concentration in particle	mol m^{-3}
a_i	initial adsorbate concentration in particle	mol m^{-3}
$a_s(T)$	temperature dependent monolayer capacity in the Langmuir equilibrium equation	mol m^{-3}
a_t	total loading of the particle	mol m^{-3}
$\bar{a}$	average adsorbate concentration in particle	mol m^{-3}
a_0^*	equilibrium adsorbate concentration	mol m^{-3}
$(\bar{a}/a_0^*)_{10}$	experimental saturation at $t = 10$ min	1
Bi_M	Biot's number for mass transfer	1
c	adsorptive concentration in the gaseous phase	mol m^{-3}
c_i	equilibrium initial adsorptive concentration	mol m^{-3}

c_R	adsorptive concentration at the particle surface	mol m^{-3}
c_o	constant adsorptive concentration in the bulk flow	mol m^{-3}
C_p	specific heat of sorbent	J kg^{-1} K^{-1}
d_P	diameter of spherical particle	m
D_A	effective surface diffusivity	m^2 s^{-1}
D_A^*	apparent surface diffusivity	m^2 s^{-1}
D_B	bulk diffusivity	m^2 s^{-1}
D_K	Knudsen diffusivity	m^2 s^{-1}
D_P	effective pore diffusivity	m^2 s^{-1}
D_P^*	apparent pore diffusivity	m^2 s^{-1}
h	film heat transfer coefficient	J m^{-2} s^{-1} K^{-1}
h_A	adsorbate molar enthalpy in the adsorbed phase	J mol^{-1}
h_M	film mass transfer coefficient	m s^{-1}
h_P	adsorptive molar enthalpy in the gaseous phase	J mol^{-1}
h_s	volume enthalpy of solid	J m^{-3}
h_t	total volume enthalpy of particle	J m^{-3}
$\boldsymbol{H}_F$	heat flux in the film	J m^{-2} s^{-1}
$\boldsymbol{H}_I$	total heat flux in the particle	J m^{-2} s^{-1}
$-\Delta H$	heat of adsorption	J mol^{-1}
$\boldsymbol{J}_A$	surface diffusion molar flux	mol m^{-2} s^{-1}
$\boldsymbol{J}_F$	molar flux in the film	mol m^{-2} s^{-1}
$\boldsymbol{J}_I$	total molar flux in the particle	mol m^{-2} s^{-1}
$\boldsymbol{J}_P$	pore diffusion molar flux	mol m^{-2} s^{-1}
$K(T)$	temperature dependent equilibrium parameter in the Langmuir equation	Pa^{-1}
p	partial pressure of adsorptive	Pa
r	radial coordinate in the spherical particle	m
R	radius of the spherical particle	m
Re_P	modified Reynolds' number	1
t	time	s
T	absolute temperature	K
T_i	initial temperature	K
T_R	temperature at the particle surface	K
T_o	temperature in the bulk flow	K
ε	porosity of particle	1
λ_e	effective thermal conductivity of sorbent particle	J m^{-1} s^{-1} K^{-1}
μ	labyrinth factor	1
ϱ	density of sorbent particle	kg m^{-3}

References

1. Ruthven, D. M. and Loughlin, K. F., *Can. J. Chem. Eng. 50,* 550 (1972).
2. Wakao, N. and Smith, J. M., *Chem. Eng. Sci. 17,* 825 (1962).
3. Ruckenstein, E., Vaidyanathan, A. S., and Youngquist, G. R., *Chem. Eng. Sci. 26,* 1305 (1971).

4. Ruthven, D. M. and Loughlin, K. F., *Chem. Eng. Sci. 26,* 577 (1971).
5. Neretnieks, I., *Chem. Eng. Sci. 31,* 107 (1976).
6. Bird, R. B., Stewart, W. E., and Lightfoot, E. N., *Transport Phenomena.* J. Wiley and Sons, New York, 1965.
7. Weber, T. W. and Chakravorti, R. K., *AIChE J. 20* (2), 228 (1974).
8. Rajniak, P., Molčan, M., and Žemlička, A., *Chem. Zvesti 36,* 721 (1982).
9. Rajniak, P., Brunovská, A., and Ilavský, J., *Chem. Zvesti 36,* 733 (1982).
10. Villadsen, J. and Michelsen, M. L., *Solution of Differential Equation Models by Polynomial Approximation.* Prentice Hall, New Jersey, 1978.
11. Marcussen, L., *Chem. Eng. Sci. 29,* 2061 (1974).
12. Suzuki, M. and Kawazoe, K., *J. Chem. Jap. 7,* 346 (1974).
13. Buchholz, H. and Krückels, V., *Verfahrenstechnik 10,* 290 (1976).
14. Marcussen, L., *Chem. Eng. Sci. 25,* 1487 (1970).
15. Neretnieks, I., *Chem. Eng. Sci. 31,* 1029 (1976).
16. Fritz, W., Merk, V., and Schlünder, E. U., *Chem. Eng. Sci. 36,* 731 (1981).
17. Satterfield, C. N., *Mass Transfer in Heterogeneous Catalysis.* Mass: MIT Press, Cambridge, 1970.

Translated by P. Rajniak